Journal of the Korean Nuclear Society
Volume 31, Number 6, pp.618~630, December 1999

A Theoretical and Experimental Study of the Steam Condensation Effect on the CCFL in Nearly Horizontal Two-phase Flow

Moon-Hyun Chun and Seon-Oh Yu
Korea Advanced Institute of Science and Technology
373-1, Kusong-Dong, Yusong-Gu, Taejon, 305-701, Korea
soyu1004@nesun1.kaist.ac.kr

(Received July 28, 1999)

Abstract

An analytical model that includes the steam condensation effect has been derived and a parametric study has been performed. In addition, a series of experiments were performed and a total of 34 experimental data for the onset of CCFL in nearly horizontal countercurrent two-phase flow have been obtained for various flow rates of water. Comparisons of the present CCFL data with slug formation models show that the agreement between the present as well as the existing model and the data is about the same. However, the deviation between the Taitel and Dukler' s model predictions and the data is the largest when $j_f < 0.04$ m/s. A parametric study of the effect of the steam condensation using the present model shows that, when all local conditions are similar, the model predicted local gas velocities that cause the onset of flooding are slightly lower when condensation occurred. Based on the visual observation and the evaluation of the present work, it has been concluded that the criterion derived for the onset of slug flow can be directly used to predict the onset of inner flooding in nearly horizontal two-phase flow within the experimental ranges of the present work.

Key Words : onset of CCFL, steam condensation effect, onset of slug flow, steam-water stratified countercurrent two-phase flow

1. Introduction

When gas flows over a liquid surface with sufficiently large relative velocity in a horizontal pipe or duct, the gas-liquid interface becomes wavy, with further increases in the gas or liquid velocity, eventually the waves become unstable and grow to block the whole cross section. As a result, the transition from stratified wavy flow to slug flow occurs. Over the last 30 years, a number of experimental and theoretical studies have been performed concerning the transition to slug flow. An equal amount of studies on the countercurrent flow limiting (CCFL) phenomenon generally known as "flooding" has also been conducted during the same period. Except for the most recent works published after 1990, most of the existing theories on the transition to slug flow

Table 1. Summary of Analytical Criterion for the Onset of Slug Flow

Authors	Criterion Equation		Dimensionless Form ($V_g >> V_f$, θ=0, Duct Flow)	
Kordyban and Ranov (1970)	$(V_g - V_f) \geq K_1 \sqrt{\frac{\rho_f g}{\rho_g \kappa}}$ $K_1 = \sqrt{\frac{1}{\coth(\kappa H_g - 0.9) + 0.45\coth^2(\kappa H_g - 0.9)}}$	(i-a)	$j_g^* \geq K_1 \frac{\alpha}{\sqrt{\kappa H}}$	(i-b)
Wallis and Dobson (1973)	$(V_g - V_f) = 0.5\sqrt{\frac{(\rho_f - \rho_g) g H_g}{\rho_g}}$	(ii-a)	$j_g^* = 0.5\alpha^{3/2}$	(ii-b)
Taitel and Dukler (1976)	$V_g > \left(1 - \frac{H_f}{D}\right)\sqrt{\frac{(\rho_f - \rho_g)}{\rho_g}\frac{g A_g \cos\theta}{dA_f/dH_f}}$	(iii-a)	$j_g^* > \alpha^{5/2}$	(iii-b)
Gardner (1979)	$1 - \left(1 - \frac{1}{\rho^*}\right)\frac{H_f}{H} = \frac{4F_{1\Delta} - 3(3+\rho^*)F_{1\Delta}^2 + 4(1+\rho^*)F_{1\Delta}^3}{2 - 2(3+\rho^*)F_{1\Delta} + 3(1+\rho^*)F_{1\Delta}^2}$ $F_{1\Delta} = \sqrt{\frac{\rho_g}{(\rho_f - \rho_g) g H}}(V_g - V_f),\ \rho^* = \left(\frac{\rho_f}{\rho_g}\right)^{1/2}$	(iv-a)	$j_g^* = F_{1\Delta}\alpha$	(iv-b)
Mishima and Ishii (1980)	$(V_g - V_f) \geq 0.487\sqrt{\frac{(\rho_f - \rho_g) g H_g}{\rho_g}}$	(v-a)	$j_g^* \geq 0.487\alpha^{3/2}$	(v-b)
Chun et al. (1996)	$V_{g,crit} = \sqrt{\frac{(\rho_f - \rho_g) g H_g C_{P,crit}}{\rho_g}\frac{\sqrt{4/\pi + f_i} - 1}{4/\pi + f_i - 1}}$ $C_{P,crit}$ = geometric factor at critical condition = 1 for a duct flow.	(vi-a)	$(j_g^*)_{crit} = \frac{\sqrt{4/\pi + f_i} - 1}{4/\pi + f_i - 1}\alpha^{3/2}$ $\cong 0.470\alpha^{3/2}$ when $f_i = 0$	(vi-b)

have been closely reviewed by Kordyban [1]. For the purpose of the present work, therefore, only the major analytical models that have been selected for comparative purposes with the present model are summarized in Table 1 [2-7]. As shown in Table 1, most of the models proposed for the transition to slug flow in horizontal two-phase flow are expressed in terms of void fraction and the non-dimensional superficial velocity of the gas phase.

One of the most important applications of "the transition criterion to slug flow" in nuclear reactor systems is that it is used as "the criterion for initiation of the condensation-induced waterhammer (CIWH)" which is known as the most damaging form of waterhammer in pressurized water reactors (PWRs): The water slug formation criterion is directly used as the criterion for the onset of the CIWH [8].

In relation to the present work, the observations made by Choi and NO [9] are particularly noteworthy. Based on the visual observations, they suggested two mechanisms governing the transition to flooding in nearly horizontal pipes: "inner flooding" and "entrance flooding". The inner flooding is initiated by unstable wave growth, i.e., slugging, at the inner location of the pipe. The entrance flooding, on the other hand, is always observed to take place at the entrance of the water flow without slugging. They further noted that the flooding is initiated by sudden growth of waves that are already in the pipe before the onset of flooding. The waves created by the air shear force continue to grow until

flooding occurs, propagating toward the entrance of the water flow. The location of the onset of flooding varies from the entrance to the exit of the water flow depending on the water flow rate and the inclination angle. Also, the transition criterion for the onset of flooding is approximately consistent with that of the slug formation.

With regard to nuclear reactor safety, in particular, the most typical events where the CCFL can occur in the hot legs of PWRs are the reflood phase of a large break loss of coolant accident (LOCA) and the reflux cooling in a small break LOCA. In the postulated light water reactor LOCA, the emergency core cooling (ECC) water is subcooled, and steam condensation that reduces the effective upward steam flux may affect the CCFL characteristics. As pointed out by Tien [10], the existing flooding or CCFL correlations are all semi-empirical in nature, and in the absence of steam condensation, the most widely used CCFL correlation has been the Wallis correlation [11]. Using a simple analytical model to analyze the effect of steam condensation on the CCFL phenomenon, Tien [10] has shown that steam condensation affects greatly the CCFL phenomenon and may significantly enhance the CCFL break-down.

From the review of the existing works on the transition criterion to slug flow and the onset of CCFL phenomenon in horizontal or nearly horizontal two-phase flow, in particular, the following two questions immediately arise:

(1) How can we evaluate quantitatively the effects of steam condensation on the transition from stratified flow to slug flow and also on the CCFL phenomenon?

(2) Can we simply use "the transition criterion from stratified flow to slug flow" to predict the onset of CCFL at least in nearly horizontal two-phase flow?

To analyze the effect of steam condensation on the transition to slug flow and on the CCFL phenomenon, an analytical model that includes the steam condensation effect has been derived and a parametric study has been performed in the present work. In addition, a series of experiments were performed and a total of 34 experimental data for the onset of CCFL in nearly horizontal (0.25° and 0.5° from the water inlet) countercurrent two-phase flow (air-water and steam-water) have been obtained for various flow rates of water. The purpose of this paper is to present the results of these analytical and experimental studies along with the discussions on the above two questions posed.

2. Analysis

To derive a slug formation model including the effect of steam condensation, the countercurrent stratified wavy flow shown in Fig. 1 is considered. When the steam flows over a wavy liquid surface with a phase change at the interface, the wave grows by the Bernoulli force due to the pressure difference over the wave crest: This appears as the kinetic energy increase of the gas phase over the wave crest. The wave also grows due to the shear stress on the front of the wave crest and the momentum loss of the condensing steam. Against these forces, there is a stabilizing force due to the gravity. Therefore, the total energy balance over the wave crest can be expressed as follows:

$$E_p = \Delta E_k + W_r + W_c \tag{1}$$

where E_p = Total potential energy of the wave crest,

ΔE_k = Net kinetic energy increase of the gas over the wave crest,

W_r = Work done by the shear stress on the front surface of the wave crest, and

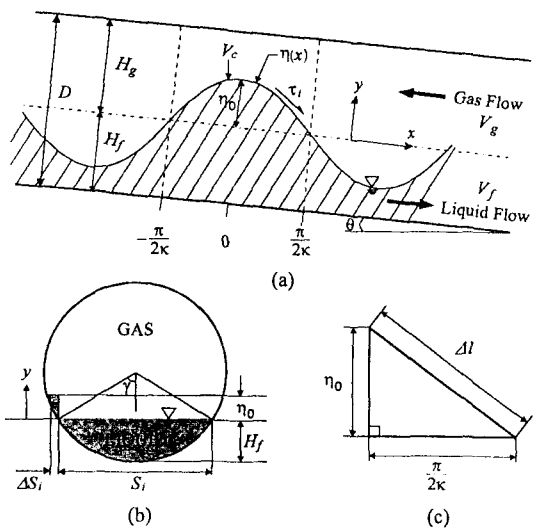

Fig. 1. Countercurrent Stratified Wavy Flow Models for Analysis

W_c= Work done by the momentum loss of the condensing steam.

If W_c were not considered, Eq. (1) reduces to the same form of Chun et al. [7]. It is assumed that the interfacial wave is of the sinusoidal form as follows:

$$\eta(x) = \eta_0 \cos \kappa x \tag{2}$$

In addition, the gas velocity in the x-direction is expressed in terms of the wave displacement η, and the velocity potential function ϕ_v, introduced by Lamb [12] as follows:

$$\phi_v = -V_g x + c_g \cosh \kappa(y - H_g) \sin \kappa x \tag{3}$$

where c_g is an arbitrary constant. Using the definition of a gas velocity $\left(u_x = -\frac{\partial \phi_v}{\partial x}\right)$ and the mass balance equation over the wave crest, the gas velocity can be expressed as

$$u_x = V_g \left[1 - \frac{\eta_0 \kappa}{\sinh \kappa(\eta_0 - H_g)} \cosh \kappa(y - H_g) \cos \kappa x\right] \tag{4}$$

2.1. Total Potential Energy of the Wave Crest

The total potential energy of the wave crest (per unit thickness), E_p, is simply due to the elevated water from the undisturbed interface and can be expressed as

$$E_P = \int_{\frac{\pi}{2\kappa}}^{\frac{\pi}{2\kappa}} \int_0^{\eta} y \rho_f g \cos\theta (S_i + \Delta S_i) dy dx = \frac{\pi}{4\kappa} \rho_f g \cos\theta \eta_0^2 S_i C_P \tag{5}$$

where Δs_i is related only to pipe flow as shown in Fig. 1(b) and becomes zero for rectangular duct. In addition, the geometric factor, C_p, for pipe flows is given by

$$C_P \equiv 1 + \frac{32}{9\pi} \frac{\eta_0}{S_i} \frac{D}{S_i} \left(1 - \frac{2H_f}{D}\right) \tag{6}$$

For rectangular duct flows, C_p is equal to unity.

2.2. Net Kinetic Energy Increase of the Gas Phase

The net kinetic energy increase of the gas phase over the wave crest, ΔE_k, may be considered to be the difference between the 'kinetic energy of the gas with the wave crest' and the 'kinetic energy of the gas without the wave crest', and can be written as

$$\Delta E_k = \frac{1}{2} \rho_g S_i \int_{\frac{\pi}{2\kappa}}^{\frac{\pi}{2\kappa}} \int_{\eta}^{H_g} u_x^2 dy dx - \frac{1}{2} \rho_g S_i \int_{\frac{\pi}{2\kappa}}^{\frac{\pi}{2\kappa}} V_g^2 H_g dx = \frac{\pi}{4\kappa} \rho_g V_g^2 S_i \eta_0 \left[\frac{4}{\pi} + \frac{\eta_0}{H_g - \eta_0}\right] \tag{7}$$

2.3. Total Work Done by Interfacial Shear Stress

During the time required to travel the distance of $\pi/2k$ in the x-direction with velocity V_g, the total

work done on the front surface of the wave crest by the interfacial shear stress, W_τ, is given by

$$W_\tau = \int_t \tau_{i,y} S_i \Delta l V_g dt = \frac{\pi}{4\kappa} f_i \rho_g V_g^2 S_i \eta_0 \quad (8)$$

where $\tau_{i,y}$ is the interfacial shear stress in the y-direction and Δl is the length of wave crest where the interfacial shear stress acts, modeled as a triangle.

2.4. Total Work Done by Momentum Loss of Condensing Steam

It is assumed that the condensing steam becomes stagnant at the interface when the phase change takes place: The resulting force due to the momentum loss of the condensing steam acts on the liquid phase. It is also assumed that the effect of the wave profile on the condensation heat transfer is small enough to be neglected and the interfacial heat transfer coefficient h_c is considered to be uniform throughout the wave length. The normal component of the momentum of the condensing steam can be approximated by [13]:

$$F_c = \frac{1}{2}\rho_g V_c^2 \left(\frac{d\eta}{dx}\right) \quad (9)$$

where V_c is the average velocity of the condensing steam. Since relatively deep water waves are concerned with slug formation as Mishima and Ishii [6] noted, it is assumed that $\kappa\eta_0=1.0$. Then, the work done by the momentum loss of the condensing steam, W_c, can be obtained as

$$W_c = \int F_c (S_i 2\Delta l) d\eta = 3.72\left(\frac{\pi}{4\kappa}\rho_g V_c^2 S_i \eta_0\right) \quad (10)$$

2.5. Condition for Transition from Stratified Flow to Slug Flow

The critical gas velocity, $V_{g,crit}$, at which the transition from stratified flow to slug flow occurs can be derived as follows: First, substituting Eqs. (5), (7), (8) and (10) into Eq. (1), the following total energy balance equation over the wave crest is obtained:

$$\frac{\pi}{4\kappa}\rho_f g \cos\theta \eta_0^2 S_i C_P = \frac{\pi}{4\kappa}\rho_g V_g^2 S_i \eta_0 \left[\frac{4}{\pi} + \frac{\eta_0}{H_g - \eta_0} + f_i\right] + 3.72\left[\frac{\pi}{4\kappa}\rho_g V_c^2 S_i \eta_0\right] \quad (11)$$

Defining the dimensionless wave height ($\eta_0^* \equiv \eta_0/H_g$), Eq. (11) can be rewritten as:

$$\eta_0^{*2} - \left[(1+C_c) + C_\eta\left(\frac{4}{\pi} + f_i - 1\right)\right]\eta_0^* + C_\eta\left(\frac{4}{\pi} + f_i\right) + C_c = 0 \quad (12)$$

where

$$C_\eta \equiv \frac{\rho_g}{\rho_f}\frac{V_g^2}{gH_g \cos\theta C_P} \quad (13)$$

$$C_c \equiv \frac{\rho_g}{\rho_f}\frac{3.72V_c^2}{gH_g \cos\theta C_P} \quad (14)$$

Since the wave height increases with the increase in the gas velocity, the physically meaningful solution of Eq. (12) for the wave height in wavy flow is given by

$$\eta_0^* = \frac{1}{2}\left[(1+C_c) + C_\eta\left(\frac{4}{\pi} + f_i - 1\right) - \sqrt{\left\{(1+C_c) + C_\eta\left(\frac{4}{\pi} + f_i - 1\right)\right\}^2 - 4\left\{C_\eta\left(\frac{4}{\pi} + f_i\right) + C_c\right\}}\right] \quad (15)$$

When the maximum wave height is reached by further increasing the gas velocity, the flow may be forced to change from stratified wavy flow to slug flow. In view of the expression for the wave height, Eq. (15), the onset of slugging (i.e., the

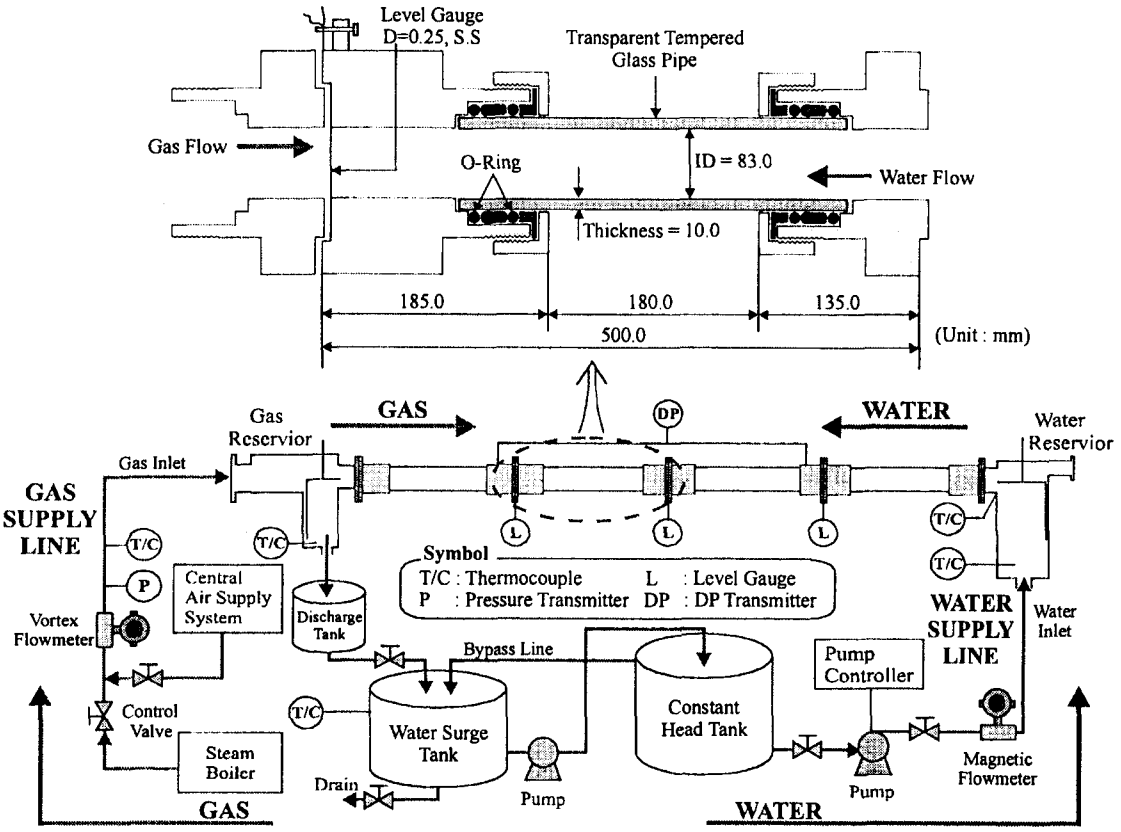

Fig. 2. Schematic Diagram of Experimental Apparatus

transition from stratified wavy flow to slug flow) occurs when the terms in the square root in Eq. (15) becomes zero. Then, the critical gas velocity $V_{g,crit}$ at which the transition from stratified wavy flow to slug flow occurs can be obtained as follows:

$$V_{g,crit} = \sqrt{\frac{\rho_f g H_g \cos\theta C_{P,crit}}{\rho_g}} \frac{\sqrt{\left(\frac{4}{\pi}+f_i\right)(1-C_c)+C_c}-1}{\frac{4}{\pi}+f_i-1} \quad (16)$$

where $C_{p,crit}$ is the critical value for C_p in Eq. (6). The criterion for the onset of slugging, Eq. (16), derived in the present work reduces to the same form obtained by Wallis and Dobson [3], Mishima and Ishii [6] when the effects of both the interfacial shear stress and the steam condensation are neglected, i.e., (f_i = 0) and (C_c = 0), and the geometric factor is taken as unity ($C_{p,crit}$ =1) as in the case of rectangular duct flows. Equation (16) becomes identical to the expression derived by Chun et al. [7] when the effect of the steam condensation is omitted.

3. Experiments

A series of experiments were performed and a total of 34 experimental data for the onset of CCFL (17 for the steam-water flow and 17 for the air-water flow condition) in nearly horizontal countercurrent two-phase flow have been obtained

Table 2. Test Matrix for Present Experiments

	Test Section			j_f [m/s]	Re_f	j_g [m/s]	No. of Data Points
	Diameter	Length	Inclination Angle				
Air/Water Test	0.083 m	2.2 m	0.25°	0.02 ~0.10	1057 ~9256	0~5.00 (up to the CCFL)	17
Steam/Water Test	0.083 m	2.2 m	0.5°	0.02 ~0.10	1628 ~12474	0~7.67 (up to the CCFL)	17
Total number of experimental data							34

for various flow rates of water. The test matrix is shown in Table 2.

3.1. Experimental Apparatus

A schematic diagram of the experimental apparatus is shown in Fig. 2. The main components of the system were ① the test section, ② the air, steam, and water supply system, ③ sensors and devices to measure the water level and flow rates, and ④ the data acquisition system.

The test section is slightly inclined (0.25° and 0.5° from the water inlet) and consists of four transparent tempered glass pipes which are connected in series by flanges. The total length and inside diameter of the horizontal channel are 2.2m and 0.083m, respectively. While the compressed air was supplied by the central air supply system, the saturated steam was supplied by a 200kW electric steam boiler. Filtered tap water was pumped from the water surge tank to the test section and uniform flow of water was achieved by installing a honeycomb in the water reservoir. The water surge tank (1.0 m^3) was used to provide a steady flow rate of water flowing into the test section. The flow rates of steam (or air) and water were measured by a vortex and a magnetic flowmeters, respectively: The accuracy of the vortex and the magnetic flowmeters were within ±1.0% and ±0.5%, respectively. The inlet temperatures of steam (or air) and water were also measured by *k*-type thermocouples installed at the downstream of the vortex flowmeter and inside the water reservoir, respectively. The instantaneous water level was evaluated by measuring the electrical resistance which varies according to the changes in the water level difference between two vertical parallel electrodes inserted in the test section. The electrodes consisted of two stainless steel wires of 0.25 mm in diameter, mounted vertically in the test section about 5 mm apart in a plane perpendicular to the direction of the flow. The level sensors were calibrated for each run and also checked repeatedly during the test: The response of this level gauge was quite linear and the average standard deviation was about 0.5 mm.

3.2. Test Parameters and Test Procedure

The major test parameters in the present work were the inlet flow rates of water and air (for air-water test) and steam (for steam-water test) and the water level. A total of 34 runs were made for various combinations of test parameters under atmospheric pressure condition as summarized in Table 2. The range of superficial velocity of water (i.e., j_f) was 0.02 0.10 m/s, whereas those of steam and air (i.e., j_g) were 0.00~7.67 m/s and

Table 3. Comparison of $(j_g)_{crit}$ Values With and Without Condensation Factor C_c

	System Conditions			j_f = 0.193m/s		
	P [MPa]	D [m]	ΔT_{sub} [℃]	$(j_g)_{crit}$ [m/s]		(②-①)/① [%]
				① $C_c>0$	② C_c = 0	
1	0.1	0.3	90	5.300	5.513	3.87
	1.5	0.3	90	2.342	2.664	12.10
2	1.5	0.05	90	0.479	0.480	0.19
	1.5	0.3	90	2.342	2.664	12.10
3	1.5	0.3	10	2.628	2.636	0.32
	1.5	0.3	90	2.342	2.664	12.10

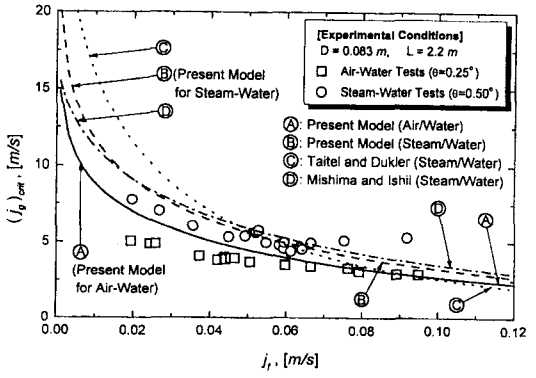

Fig. 3. Dimensional j_g Versus j_f Curves for Present CCFL Data and Model Predictions

0.00~5.00 m/s, respectively.

The experimental procedure for a given test is as follows: (1) The inlet water flow rate was first set to a specified value. (2) The air (or steam) flow rate was then increased in small steps until the onset of CCFL (or slugging) occurred. (3) After allowing a sufficient time to reach a quasi-steady state, the time averaged water level and flow rates were taken. The same procedure has been repeated for all the tests.

The onset of CCFL was readily determined by direct visual observation as a slight increase in air (or steam) flow rate (at the onset of CCFL) resulted in a dramatic change in the flow pattern. In addition, the reproducibility of the present test data has been confirmed by repeating the same test three times under typical test conditions: The ranges of standard deviation of j_f and $(j_g)_{crit}$ evaluated for two sets of reproducibility tests were 0.0007~0.002 and 0.18~0.20, respectively.

4. Results and Discussion

4.1. Comparisons of the Present CCFL Data with Slug Formation Models

Present experimental CCFL data for both steam-water and air-water countercurrent two-phase flows are first presented in the form of dimensional j_g versus j_f curves along with the predictions of the present and the typical existing models proposed for the onset of slug flow in Fig. 3. From this figure the following observations can be made:

(1) The agreement between the data and the model predictions is fairly good for j_f > ~0.03 m/s.

(2) For a given water flow rate (or the superficial liquid phase velocity, j_f), the critical gas flow rates (or the superficial gas phase velocity, $(j_g)_{crit}$) at which CCFL occur for steam-water flow are larger than those for air-water flow. The main reason for this can be explained using Eq. (16)

as follows: While the condensation effect of steam on the CCFL (represented by C_c in Eq. (16)) at relatively low system pressure is very small (e.g., $C_c = 9.47\times10^{-4}$ when $j_f = 0.041 m/s$, $P = 0.1$MPa, $D = 0.083m$, $\Delta T_{sub} = 70℃$), the density ratio of the water and the steam is larger than that of water and air:

$$(\rho_f / \rho_g)_{\text{Steam-Water}} > (\rho_f / \rho_g)_{\text{Air-Water}} \quad (17)$$

Therefore, $(j_g)_{crit}$ for steam-water flow is greater than that for air-water flow.

(3) The agreement between the present as well as the existing model and the data is about the same, except that the deviation between the Taitel and Dukler' s model predictions and the data is the largest when j_f is smaller than 0.04 *m/s*.

4.2. Effect of Steam Condensation on the Onset of CCFL

It is not quite possible to quantitatively evaluate the effect of steam condensation on the CCFL by any experimental procedure. However, the present model can be used to determine the steam condensation effect on the CCFL as follows: In the present criterion used in the analysis of the onset of CCFL, Eq. (16), the contribution of steam condensation on the CCFL is represented by the dimensionless condensation factor C_c defined by Eq. (14). Therefore, to quantitatively evaluate the steam condensation effect on the onset of CCFL, the critical gas velocities are calculated using Eq. (16) with and without steam condensation factor C_c. The results of sample quantitative estimation of the steam condensation effect on the CCFL are summarized in Table 3. The predicted critical gas velocities with the steam condensation factor are lower than those without the steam condensation factor.

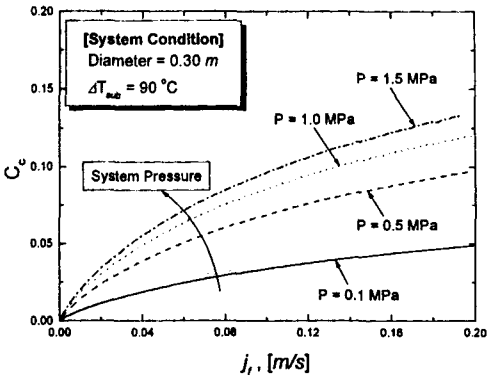

(a) Effect of system pressure

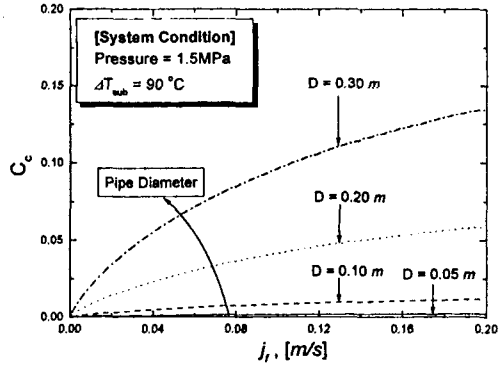

(b) Effect of pipe diameter

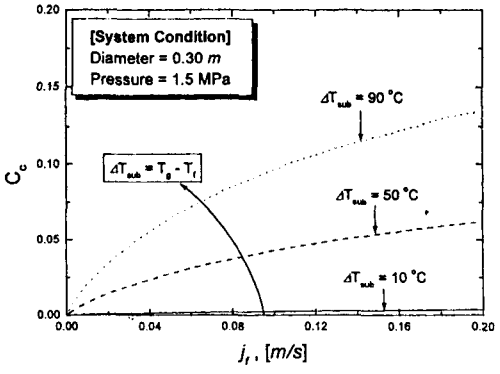

(c) Effect of subcooling

Fig. 4. Effects of Three Parameters on the Steam Condensation Factor C_c

In addition, the effects of three major parameters (i.e., P, D and ΔT_{sub}) on the CCFL are indirectly examined by evaluating the dependency of the steam condensation factor on each of the three major parameters: The parametric effects of the system pressure, the pipe diameter, and the subcooling on the condensation factor C_c are shown as C_c versus j_f curves in Figs. 4(a)~(c). These figures show that when each system parameter (i.e., the system pressure, the pipe diameter, and the subcooling) is increased, the condensation factor C_c increases without any exception. This means that when the system pressure, or the pipe diameter, and/or the subcooling is increased, the effect of steam condensation on the onset of CCFL also increases.

4.3. Applicability of the Slug Formation Model to Predict the Onset of CCFL in Nearly Horizontal Two-phase Flow

In the case of "inner flooding", the formation of a water slug was observed at the inner location of the pipe just before the onset of flooding. This means that "the slug formation" in nearly horizontal two-phase flows can be considered as "a precursor to an inner flooding" phenomenon. Also, comparisons of the present CCFL data with slug formation models shown in Fig. 3 clearly show that the criterion for the onset of slug flow can be directly used to predict the onset of CCFL in nearly horizontal two-phase flow within the range of the present experiments. Then, what accounts for the almost exclusive use of the Wallis type flooding correlation in the flooding analysis up to now? A possible answer is provided in the following.

In the absence of steam condensation, the most widely used Wallis correlation for CCFL is given by:

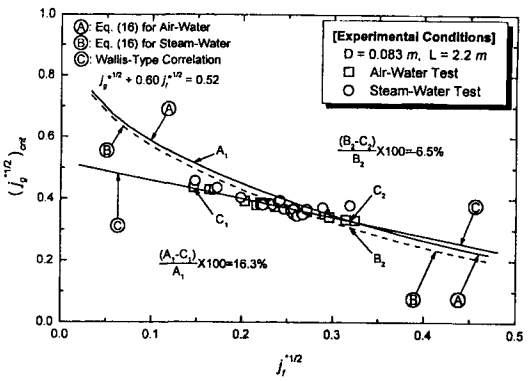

Fig. 5. Comparison of the Critical Gas Velocities, $(j_g^{*1/2})_{crit}$ Predicted by Eq. (16) and Eq. (19)

$$j_g^{*1/2} + m\, j_f^{*1/2} = C \tag{18}$$

where $m \cong 1.0$ and $C \cong 0.7 \sim 1.0$, both constants are determined from experiments. As can be seen in Eq. (18), the Wallis type flooding or CCFL correlations are semi-empirical in nature. Using the present experimental data (a total of 34) for the onset of CCFL, a flooding correlation has been developed in terms of Wallis parameters as follows:

$$j_g^{*1/2} + 0.60 j_f^{*1/2} = 0.52 \tag{19}$$

Figure 5 shows the critical gas velocities at which inner flooding occurs for various water flow rates and compares the data with predictions of Eq. (19) and the present slug formation model. As can be seen in Fig. 5, Eq. (19) agrees with the data more closely than the slug formation model. The reason for this is obvious: While Eq. (19) was obtained by fitting Eq. (18) to the present CCFL data, the slug formation model was derived theoretically. Based on these observations, the following recommendations are made:

(1) The criterion derived for the onset of slug flow

can be directly used to predict the onset of inner flooding in nearly horizontal two-phase flow.

(2) However, when a more accurate CCFL correlation is needed, one can develop a Wallis type flooding correlation at the expense of a little more effort.

5. Conclusions

In an effort to analyze the effect of steam condensation on the transition from stratified flow to slug flow and on the CCFL phenomenon, an analytical model that includes the steam condensation effect has been derived and a parametric study has been performed. In addition, a series of experiments were performed and a total of 34 experimental data for the onset of CCFL in nearly horizontal (0.25° and 0.5° from the water inlet) countercurrent two-phase flow (air-water and steam-water) have been obtained for various flow rates of water. From the present theoretical and experimental studies the following conclusions can be made.

First, comparisons of the present CCFL data with slug formation models show the following: For a given water flow rate (or j_f), the critical gas flow rates (or $(j_g)_{crit}$) at which CCFL occurs for steam-water flow are larger than those for air-water flow. The agreement between the present as well as the existing model and the data is about the same, except that the deviation between the Taitel and Dukler' s model predictions and the data is the largest when $j_f < 0.04$ *m/s*.

Second, results of a parametric study of the effect of condensation using the present model show that, when all local conditions are similar, the model predicted local gas velocities that cause the onset of flooding were slightly lower when condensation occurred.

Third, based on the experimental observation and the theoretical evaluation of the applicability of the slug formation model to predict the onset of CCFL in nearly horizontal two-phase flow the following conclusions can be made: The slug formation in nearly horizontal two-phase flows can be considered as "a precursor to an inner flooding". Therefore, within the ranges of flow parameters of the present experiment, the criterion derived for the onset of slug flow can be directly used to predict the onset of inner flooding in nearly horizontal two-phase flow. However, when a more accurate CCFL correlation is needed, one can develop a Wallis type semi-empirical flooding correlation at the expense of a little more effort.

Acknowledgement

Authors gratefully acknowledge the financial support of the Korea Electric Power Research Institute (KEPRI) through the Center for Advanced Reactor Research at the Department of Nuclear Engineering, KAIST.

Nomenclatures

A area (m^2)
c_g constant of velocity potential function ($m^2\ s^{-1}$)
C constant in Eq. (18)
C_p geometric factor defined by Eq. (6)
C_c condensation factor defined by Eq. (14)
C_η dimensionless parameter defined by Eq. (13)
D diameter (m)
E_p total potential energy of the wave crest (N m)
ΔE_k net kinetic energy increase of the gas phase (N m)
f friction factor
F_c normal component of the momentum of the condensing steam ($N\ m^{-2}$)
g gravitational acceleration ($m\ s^{-2}$)

h_c average interfacial condensation heat transfer coefficient (W $m^{-2}°C^{-1}$)
H depth (m)
j superficial velocity (m s^{-1})
Δl length of wave crest (m)
L length of test section (m)
m constant in Eq. (18)
P pressure (Pa)
Re Reynolds number
S perimeter (m)
t time (sec)
ΔT_{sub} subcooling (°C)
u_x local gas velocity (m s^{-1})
V mean velocity (m s^{-1})
W_r work done by the interfacial shear stress (N m)
W_c work done by the momentum loss of the condensing steam (N m)
α void fraction
ϕ_0 velocity potential function (m^2 s^{-1})
γ angle (radian)
η displacement of wave (m)
η_0 wave amplitude (m)
κ wave number (m^{-1})
θ inclination angle (radian)
ρ density (kg m^{-3})
τ shear stress (N m^{-2})

Subscript

c condensation
crit critical
f liquid phase
g gas phase
i interface

Superscript

* dimensionless quantity

References

1. E. Kordyban, "Horizontal Slug Flow: A Comparison of Existing Theories," *ASME J. of Fluids Engineering*, **112**, 74 (1990).
2. E. S. Kordyban and T. Ranov, "Mechanism of Slug Formation in Horizontal Two-Phase Flow," *ASME J. of Basic Engineering*, **92**, 857 (1970).
3. G. B. Wallis and J. E. Dobson, "The Onset of Slugging in Horizontal Stratified Air-Water Flow," *Int. J. of Multiphase Flow*, **1**, 173 (1973).
4. Y. Taitel and A. E. Dukler, "A Model for Predicting Flow Regime Transitions in Horizontal and Near Horizontal Gas-Liquid Flow," *AIChE Journal*, **22**, 47 (1976).
5. G. C. Gardner, "Onset of Slugging in Horizontal Ducts," *Int. J. Multiphase Flow*, **5**, 201 (1979).
6. K. Mishima and M. Ishii, "Theoretical Prediction of Onset of Horizontal Slug Flow," *ASME J. of Fluids Engineering*, **102**, 441 (1980).
7. M. H. Chun, B. R. Lee, and H. Y. Nam, "Theoretical and Experimental Investigation of the Onset of Slugging in Horizontal Stratified Air-Water Countercurrent Flow," *Int. Comm. Heat Mass Transfer*, **23**, 11 (1996).
8. M. H. Chun and H. Y. Nam, "Analysis of Waterhammer Induced by Steam-Water Counterflow in a Long Horizontal Pipe," *Int. Comm. Heat Mass Transfer*, **19**, 507 (1992).
9. K. Y. Choi and H. C. NO, "Experimental Studies of Flooding in Nearly Horizontal Pipes," *Int. J. Multiphase Flow*, **21**, 419 (1995).
10. C. L. Tien, "A Simple Analytical Model for Counter-Current Flow Limiting Phenomena with Vapor Condensation," *Letters in Heat and Mass Transfer*, **4**, 231 (1977).

11. G. B. Wallis, One Dimensional Two-Phase Flow, p. 336, McGraw-Hill, Inc., New York (1969).
12. H. Lamb, Hydrodynamics, p. 370, Dover Pub. Co., New York (1945).
13. S. C. Lee, Stability of Steam-Water Countercurrent Stratified Flow, p. 152, Ph. D. thesis, Northwestern University, Evanston, Ill. (1983).